MEASUREMENT OF RATE CONSTANTS FOR THE CONTRACTILE CYCLE OF INTACT MAMMALIAN MUSCLE FIBERS

BLAIR CALANCIE AND RICHARD B. STEIN
Department of Physiology, University of Alberta, Edmonton, Canada T6G 2H7

ABSTRACT Small, random length changes were applied to bundles of intact fibers from rat and mouse extensor digitorum longus (EDL) and soleus muscles, while they were being tetanically stimulated. With increasing frequency of length changes, EDL muscle stiffness (tension change per unit change in length) increased, then decreased and increased again. The decrease was not seen in the soleus muscles. The EDL frequency- response could be well fitted by three exponential components with apparent rate constants of ~25, 150, and 500 s^{-1} at 20°C. All rate constants increased steadily with temperature and for each 10°C increase in temperature, the rates in the mouse EDL increased by a factor (Q_{10}) between 1.8 and 2.4. With tetanic stimulation, force increased nearly exponentially to a steady level with a rate constant of 24 s^{-1} at 20°C in mouse EDL muscles, and a Q_{10} of 2.4. These values correspond closely to the lowest frequency rate constant measured with length perturbations, which suggests that this process may limit the rate of rise of force in intact muscle fibers. During fatigue the high frequency and intermediate frequency rate constants declined, but the low frequency rate constant remained unchanged. These results are discussed in relation to current biochemical models for cross-bridge cycling.

INTRODUCTION

The time course in contracting muscle fibers of tension recovery after mechanical perturbations has provided much information about the processes contributing to force generation. For example, Huxley and co-workers (Huxley and Simmons, 1971; Ford et al., 1977) applied small rapid decreases in length (phase 1) to single amphibian fibers and described three distinct phases of force recovery, which they denoted phase 2 (rapid recovery of force), phase 3 (a delayed decline of force), and phase 4 (slow and final recovery of force to a steady-state value associated with the new length). Attempts have been made (Ford et al., 1977) to correlate the above mechanical events with specific biochemical processes associated with the actomyosin ATPase cycle (Lymn and Taylor, 1971; Taylor, 1979; Eisenberg and Hill, 1985).

As an alternative to perturbing muscle fibers with small step changes in length, length changes that contain a more discrete range of frequency components have also been used, such as sinusoidally varying length changes and randomly varying patterns. Inputs of this type lend themselves well to analysis of the force-generating properties of muscle fibers as a function of the stretch frequency. Kawai and his colleagues (Kawai, 1979; Cox and Kawai, 1981) have measured the mechanical frequency-response proper-

ties of skinned muscle fibers from a variety of preparations, including crustacean, amphibian, and mammalian muscles using sinusoidal length changes. These workers have also identified three distinct exponential processes with widely different rate constants (Kawai and Brandt, 1980), and have labeled these processes "A" (corresponding to phase 4 of Huxley, 1974), "B" (phase 3), and "C" (phase 2).

The third, and arguably the preferred, type of input waveform for examining the frequency-response characteristics of muscle force production to length perturbations is one made up of a wide range of frequencies simultaneously; that is, a randomly varying pattern (Barden et al., 1979; Barden, 1981). This input gives the test object's response to all frequencies of interest simultaneously, whereas numerous measurements at specific frequencies must be made sequentially using sinusoidal inputs. If the system changes between sequential measurements (e.g., during muscle fatigue), sinusoidal analysis is difficult to apply.

In this study, we have used randomly occurring length changes (Stein et al., 1986) and measured frequency-response curves and their parameters for the tension of tetanically activated muscle fibers from slow- and fast-twitch muscles of the rat and mouse. We were particularly interested in the relationship of these parameters to functional properties of contraction, such as the rate of development of force during tetani in small bundles of intact fibers. Whereas the use of intact fibers prevented us from manipulating the chemical environment bathing the fibers,

Address correspondence to Dr. R. B. Stein Department of Physiology, University of Alberta, Edmonton, Canada T6G 2H7.

as is commonly done in studies using skinned fibers (Kawai and Brandt, 1980; Goldman et al., 1984a; Cooke and Pate, 1985), the use of intact fibers has important advantages. These advantages include: (a) maintenance of the normal physiological environment in terms of ionic concentrations, allowing us to study changes in physiological conditions, (b) knowledge that the myofibrils will not undergo expansion or alterations in their relative positions, and will not be permanently affected by maximal activation, and (c) direct comparison of the rate constants measured during stretch and release to those involved in the rise and fall of tension with electrical stimulation. This paper describes the effect of (a) temperature, and (b) repeated stimulation to cause fatigue, on the frequency-response curves of intact mammalian muscle fibers. Preliminary findings have previously been reported (Calancie and Stein, 1985).

METHODS

Experiments were performed on bundles of intact muscle fibers at a variety of temperatures and states of rest or fatigue. Data for the temperature study were obtained from five bundles each of mouse and rat extensor digitorum (EDL) muscle fibers. A total of 18 bundles of mouse EDL fibers were studied during the fatigue experiments. Four preparations of fibers taken from the soleus muscle of the mouse and rat were studied. Animals were anesthetized with an intraperitoneal injection of sodium pentobarbitol (Somnotol; 60 mg/kg). The test muscle was removed and placed in Krebs-Henseleit solution (4.7 mM KCL , 118 mM NaCl, 2.5 mM $CaCl_2$, 1.2 mM $MgSO_4$, 1.1 mM KH_2PO_4, 4.5 mM $NaHCO_3$, 5.5 mM glucose). A gas mixture of 95% O_2/5% CO_2 was bubbled into the solution which brought the pH to ~7.4. Small bundles containing 10–30 fibers were dissected from the whole muscle. Although cross-sectional areas of these bundles were not accurately measured, they were typically <1 mm^2 for mouse, and somewhat larger for rat fiber bundles. In some cases preparations that included only a few fibers were examined, and upon initial examination their frequency-response properties were similar to those of larger bundles, in agreement with Kawai (1978). However, the force-generating capacity of such small bundles often degenerated within ~1 h, probably due to damage incurred during fiber dissection. Thus we limited our examination and confined our results to data obtained from somewhat larger preparations. A small amount of tendon remaining at each end of the bundle was clipped within a piece of ester-based Mylar which has very little compliance. This method of attachment helped minimize any series elasticity in the preparation and provided a stable connection of low mass. The mylar pieces were connected to the arm of a length servo (model 300H, Cambridge Technology, Inc., Cambridge, MA; nominal cutoff frequency, 300 Hz) and a force transducer hook (Cambridge model 400; DC-2,000 Hz, 1 μm/g), both of which were submerged in a second bath containing oxygenated Krebs-Henseleit solution (Fig. 1 A). Stimulation was applied via Ag/AgCl hook electrodes, using square wave stimulus pulses of ~0.5 ms duration and ~50 V. The muscle bundle was adjusted to a length (L_o) that gave the maximum twitch amplitude for single supra-maximal stimulus pulses.

Application of Random Length Changes

A detailed report of the methods for applying randomly varying length changes can be found in a recent paper from this laboratory (Stein et al., 1986). A continuous stream of the randomly varying waveforms was (a) taken from the digital-to-analog (D/A) output of a random binary switching digital circuit (Parmiggiani et al., 1981), (b) convolved with a sampling function to prevent signal aliasing (French and Holden, 1971), (c) adjusted to compensate for the mechanical properties of the length-servo, and (d) recorded on an FM instrumentation tape recorder. This
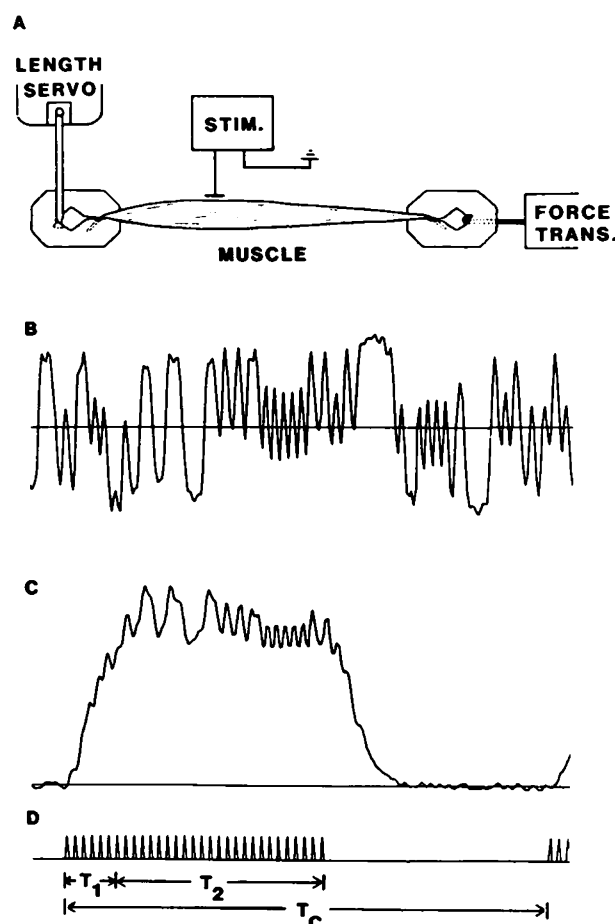

FIGURE 1 Summary of apparatus and procedures. (A) Small bundles of fibers were stimulated at 100 pulses/s, while applying random length perturbations via the servo, and recording force via the transducer. (B) Length changes were measured by the servo. They included frequencies from DC to 250 Hz, with maximum peak-to-peak amplitudes of 0.1–0.2% of L_o. (C) Output force. The increased amplitude of fluctuations during contraction reflects the increased stiffness of the bundle. The trend representing "sag" in the output was removed during analysis. (D) Trains of square-wave stimulus pulses were applied to the bundle. After an initial period to allow the force to build up (T_1), data were sampled for 1.6–10.4 s (T_2), and the stimulus stopped. Trains of stimuli were applied every 4–30 s (T_c). Length and force changes in B and C were larger than those normally used, for illustrative purposes.

resulted in waveforms, such as those shown in Fig. 1 B, whose spectrum contained frequency components from DC to a predetermined cutoff frequency, with virtually no power beyond this frequency. The cutoff frequency was varied from 30 Hz to 500 Hz, depending on the temperature used and the frequency components contained in the response of the muscle-to-length changes; frequencies greater than this 500 Hz value were not examined.

The randomly varying waveform was applied to the length servo, whose output was adjusted to produce peak-to-peak displacements of <0.2% of muscle length. The output from the servo (corresponding to the actual length changes applied to the muscle bundle) was led into one analog-to-digital (A/D) converter of a Digital Equipment Corp. (Maynard, MA) LSI 11/23 computer. Force output (Fig. 1 C) was led into a second A/D channel, and digitized values of length and force were stored on floppy disks. The data sampling rate used varied with the muscle and temperature, ranging between 1 and 16 ms.

An initial assessment of the fiber preparation was made at room

temperature. Stimuli were applied at a rate of 100 pulses/s for EDL bundles and 40 pps for soleus bundles. Stimulation and computer sampling were controlled by digital timers, as summarized in Fig. 1 D, where T_c is the cycle time, T_1 is the time allowed for the force to reach its tetanic level, and T_2 is the period of data sampling. For this initial assessment, T_c, T_1, and T_2 were 9.9, 0.3, and 2.6 s, respectively (not shown to scale in Fig. 1 D).

Analysis

Analysis consisted of computing and storing the power spectra of the length and force changes, as well as computing and plotting the frequency-response curves in various formats. For the initial assessment of EDL bundles a 2 ms sampling rate of length and force changes was used. These values were transformed using a 512 point Fast Fourier Transform (Cooley and Tukey, 1965), after removing any low frequency trends in the data (Stein et al., 1986). Even with the extra data required to remove trends, the duration of T_2 was long enough to give two determinations of the power spectra of the input length, the output force and the cross-spectrum between these two variables, using standard methods (Bendat and Piersol, 1971). The cycle was repeated several times to improve the spectral estimates.

Using a sampling rate $\Delta t = 2$ ms, the maximum usable frequency or Nyquist frequency was $1/(2\Delta t) = 250$ Hz and the minimum frequency was $1/(512\Delta t) = 0.98$ Hz. Since the lowest rate constant studied had a corner frequency of ~4 Hz ($2\pi a = 25$ s^{-1}) and the highest rate constant had a value near 80 Hz ($2\pi c = 500$ s^{-1}), this range was adequate. Division of values for the power of the cross-spectrum by that of the input

spectrum gave: (a) the magnitude of the response, representing the stiffness (change in force per unit change in length) or mechanical impedance of the bundle over a range of frequencies, and (b) the phase of muscle force with respect to input length, again for a range of frequencies. The time from the beginning of muscle stimulation to the display of a frequency response curve required <1 min to produce, and allowed an almost immediate check of the integrity of the fiber bundle. Bundles that did not show "typical" frequency-response properties upon initial assessment invariably showed a decline in the amplitude of isometric force production when tested periodically over a 1-h period. Such a deterioration was felt to reflect damage to some fibers, and the bundle was discarded. Otherwise "healthy" preparations remained viable for as many as 6–8 h after removal from the animal. If the bundle was healthy, the effects of temperature or fatigue were then studied, using methods that will be described below.

In addition the coherence of the data was calculated at each frequency, which is a normalized measure of the extent to which a linear, deterministic model accounts for the data. To the extent that there are nonlinearities or variations in output unrelated to the input, the value of coherence is lowered from its maximum value of 1 toward its minimum value of 0.

As well as plotting the frequency-response and the coherence as a function of frequency, the frequency-response curves were plotted in a Nyquist diagram (Kawai, 1979). In this diagram the real component of muscle stiffness at any frequency (i.e., the component that is in phase with the input length signal, referred to as the elastic component) is plotted on the x-axis, and the imaginary component (the component that is 90° out of phase with the input, the viscous component) is plotted on the y-axis. The viscous component is also known as "quadrature stiffness" (Goldman
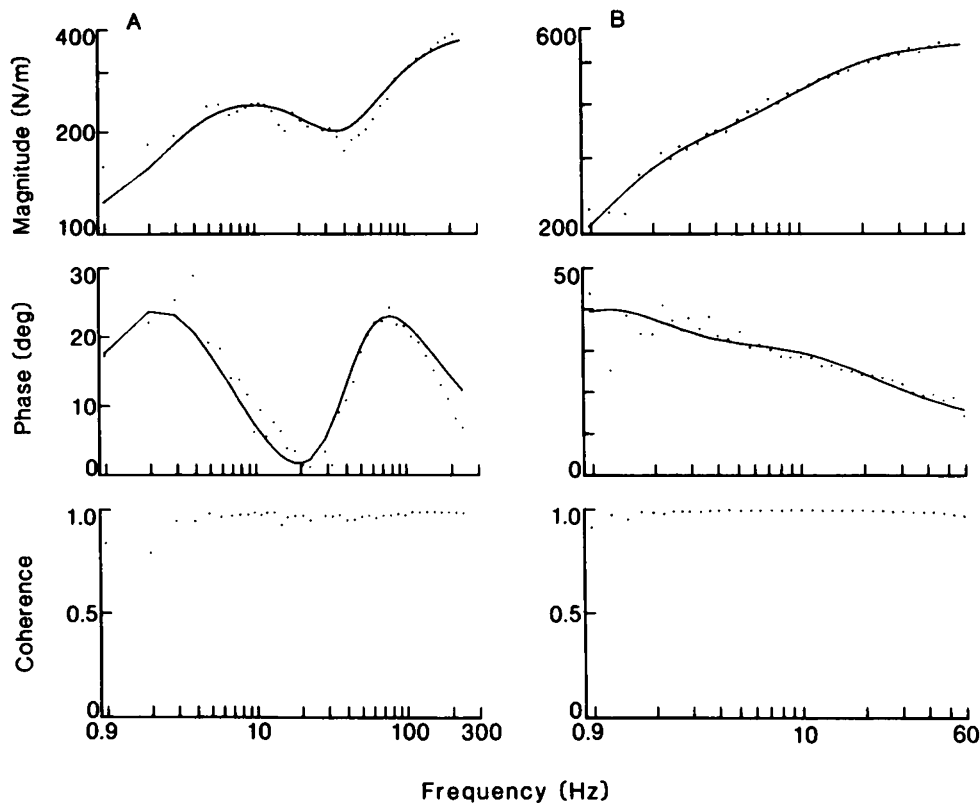

FIGURE 2   Characteristic frequency-response curves for mouse EDL (left) and soleus (right) bundles. (Top) Magnitude of dynamic stiffness. A "dip" in the curve at intermediate frequencies is seen in the EDL bundle, but not in that from soleus. (Middle) Phase of response. Force leads length at all frequencies, and EDL fibers show very clearly the peak-dip-peak response typically observed in these fibers, but not in soleus fiber bundles. (Bottom) Coherence across all frequencies was high, indicating that the muscle response to these small length perturbations can be well approximated by a linear function. The fitted curves in this and later figures were calculated by a nonlinear regression algorithm described in Methods. Length and tetanic force of EDL bundle, 7.5 mm and 55 mN; soleus bundle, 11.5 mm and 76 mN; change in length, 0.02 mm peak-to-peak.

et al., 1984a; Hibberd et al., 1985). From control theory, a visco-elastic (exponential) element in a system would exhibit a single hemi-circle in a Nyquist diagram; the observation of multiple hemi-circles in the frequency- response of muscle bundles would indicate multiple elements in the system, each with a distinctive exponential rate constant.

In this study, the rate constants were calculated by fitting the Nyquist diagram with a transfer function containing three exponential terms, and using an iteration routine to find the parameters that minimized the square of the deviations in the fitted curve from the data points (see Stein et al., 1986). The rate constants determined in this way were compared with the rising rate constant for a tetanic contraction. This rate was determined by fitting the leading edge of the tetanic force with a single exponential curve (Stein et al., 1982).

Temperature

The frequency-response characteristics during contraction were studied at a variety of temperatures, ranging between 6° and 37°C. A thermocouple measured temperature, which was varied by replacing the solution bathing the fibers with cooled or warmed Krebs-Henseleit solution. A second chamber surrounding the bath contained cooled or heated water to maintain the bath temperature. The stimulus rate was adjusted to account for differences in the fusion frequency of the muscle with different temperatures. The sampling rate was also adjusted to account for differences in the frequency components contained in the responses to length changes at different temperatures. To prevent permanent anoxic damage to the fibers, particularly at higher temperatures, and to limit increases in pH at high temperatures, attempts were made to return the bundle to room temperature as quickly as possible after each measurement. Periodic checks of the frequency-response of the bundle at the return to room temperature were made throughout the course of each experiment. At least 10 min separated each measurement at different temperatures to minimize effects of fatigue. In addition, twitch and tetanus responses of the bundle were stored for later analysis at each of the temperatures studied.

Fatigue

All fatigue studies were performed at room temperature. The stimulus parameters (Fig. 1 B) were: $T_c = 4.0$ s, $T_1 = 0.3$ s, $T_2 = 1.6$ s. This period allowed one estimate of the spectra to be calculated for each period of stimulation. The force record was sometimes stored on FM tape for later analysis of the rate of rise and fall of the tetanus. The periods of stimulation were applied for a minimum of 8 min, giving at least 120 tetanic contractions in each fatigue trial. During the experiment we stored all the raw data on a continuous file. Later, a modification of the FFT program allowed small portions of the data file, corresponding to specific tetani, to be averaged and stored as distinct spectra. This allowed comparison of the spectra at different stages of fatigue.

RESULTS

Fig. 2 shows representative tension changes of bundles of mouse EDL (*left*) and soleus (*right*) fibers at room temperature in response to small, randomly varying length changes. The random length changes contained a wide range of sinusoidal frequencies, and the frequency-response curves summarize the data at a number of frequencies. In addition to the computed points, the best-fitting curves are shown, which were determined as described by Stein et al. (1986). For the EDL, both the magnitude (*top*) and phase (*middle*) show characteristic variations with frequency. The magnitude, which has the dimensions of stiffness (change in force per unit change in length), increases initially with frequency, but then

decreases at a frequency of ~40 Hz before increasing further. The phase demonstrates a pronounced lead (force leading length) at low and high frequencies, but the phase declines to low values and sometimes lags length at intermediate frequencies.

Fig. 2 (*bottom*) shows the coherence between the input and output spectra as a function of frequency. The fact that this value is close to its maximum value of 1 at all but the lowest frequencies studied indicates that the frequency-response of the bundles was highly linear for the small amplitude length changes applied. We found that as the amplitude of the perturbations increased, the linearity of the response, as measured by the coherence function, remained high. However, the frequency-response curves failed to show a prominent "dip" in the magnitude or phase responses at stretch amplitudes exceeding ~0.8% L_o.

Frequency-response curves of soleus bundles (Fig. 2, *right*) did not show the pattern of peak-dip-peak in magnitude and phase which was characteristic of EDL bundles, in agreement with previous studies of slow-twitch fibers (Kawai and Schachat, 1984), so further analysis was restricted to EDL fiber bundles.

An alternative way of plotting the frequency-response curves is in the form of Nyquist diagrams, as shown for EDL and soleus fibers in Fig. 3. The Nyquist diagram of the EDL fibers (Fig. 3 A) shows three hemi-circles, indicating that the response in muscle force to length changes includes three exponential processes, which were centered about frequencies of 4.2, 27.1, and 82.6 Hz in this example. Following Kawai (1979), we refer to these processes as "A," "B," and "C" respectively, corresponding to Huxley's phase 4, 3, and 2 following step length changes applied to single fibers (Huxley and Simmons, 1971; Ford et al., 1977). Three hemi-circles are not apparent in the Nyquist diagram for soleus fibers (Fig. 3 B).

Fig. 4 compares the frequency-response characteristics of a mouse EDL fiber bundle during different conditions. Frequency response curves are plotted for the bundle when
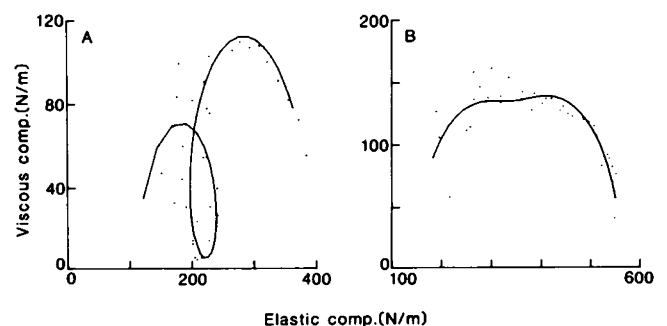

FIGURE 3 Nyquist diagrams of the same data shown in Fig. 2, for EDL (A) and soleus (B) fibers. The stiffness in phase with the length input (elastic component) is plotted on the abscissa, whereas stiffness out of phase (viscous component) is plotted on the ordinate. A distinct loop formed of three hemi-circles in the EDL curve indicates the presence of three exponential processes occurring during contraction in these fibers. No such hemi-circles are apparent in the soleus bundle.
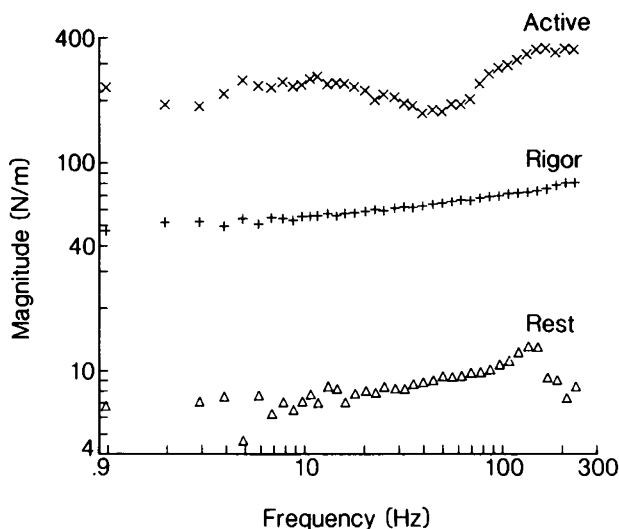
FIGURE 4 Magnitude of dynamic stiffness as a function of frequency for a mouse EDL fiber bundle preparation when actively contracting (×), when at rest (△), and after the addition of 1 mM KCN to produce partial rigor (+). Only during active contraction is the peak-dip-peak response seen, suggesting that this response reflects components of cross-bridge cycling. Length and tetanic force of the bundle were 7.0 mm and 43 mN. Peak-to-peak length changes were 0.02 mm.

unfatigued and active, at rest, and in a partial rigor state after poisoning of the Krebs- Henseleit solution bathing a fatigued preparation by the addition of 1 mM KCN. This latter state was achieved by soaking the bundle in the KCN solution for ~20 min, and probably corresponds to the "low rigor" state described by Kawai and Brandt (1976). The absence of a clear dip in stiffness at any frequency in the resting or partial rigor state indicates that the characteristic curve seen during active contraction represents processes occurring during force development by cycling of cross-bridges, and is not an artifact of the experimental procedure.

Temperature

Fig. 5 illustrates the effect of temperature on the magnitude (*left*) and phase (*right*) of a bundle of mouse EDL fibers for a range of frequencies at 10°C (*top*), 22.5°C (*middle*), and 34°C (*bottom*). The magnitude of the stiffness is highest across all frequencies at 22.5°C, but shows the same characteristic shape at all temperatures. The phase curves illustrate even more clearly that the low-frequency peak (corresponding to process "A"), the
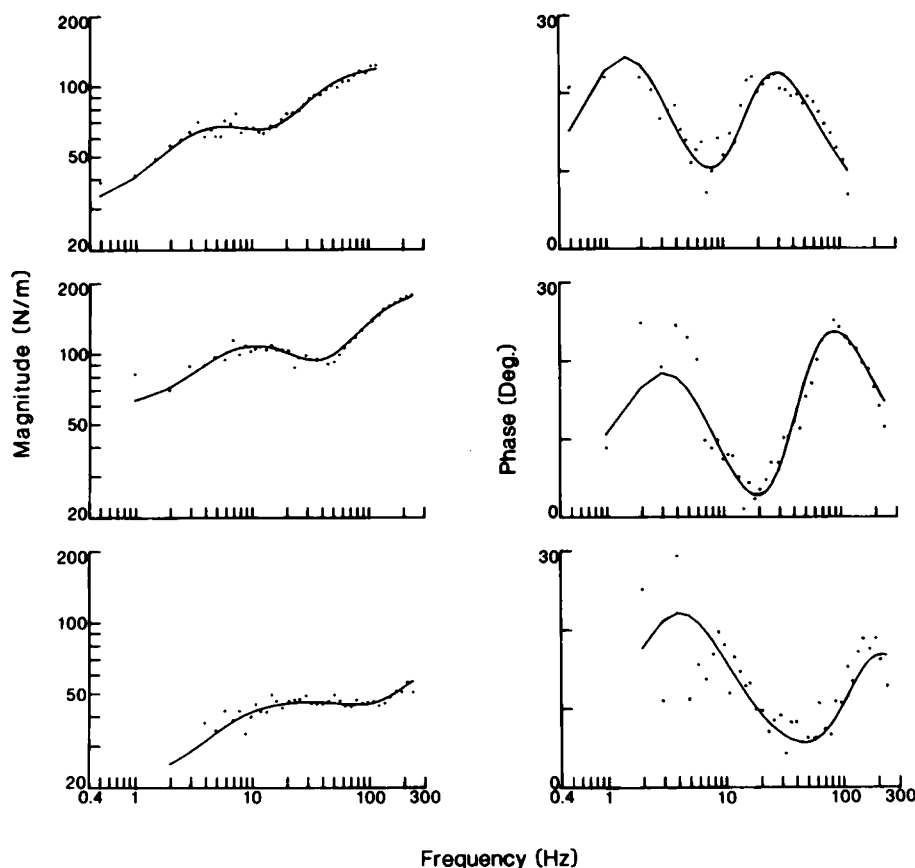

FIGURE 5 Typical frequency-response curves for the dynamic stiffness of a rat EDL bundle studied at temperatures of 10° (*top*), 22.5° (*middle*), and 34°C (*bottom*), and including the magnitude (*left*) and phase (*right*) components. The peak-dip-peak profile is apparent at all temperatures, and is best seen in the phase-frequency plots. The frequencies of the first peak (a), the dip (b), and second peak (c) all shift to the right with increasing temperature. Tetanic force of the bundle was 15 mN (10°C), 30 mN (22°C) and 26 mN (34°C) at a length of 17 mm. Peak-to-peak length changes were 0.10 mm.
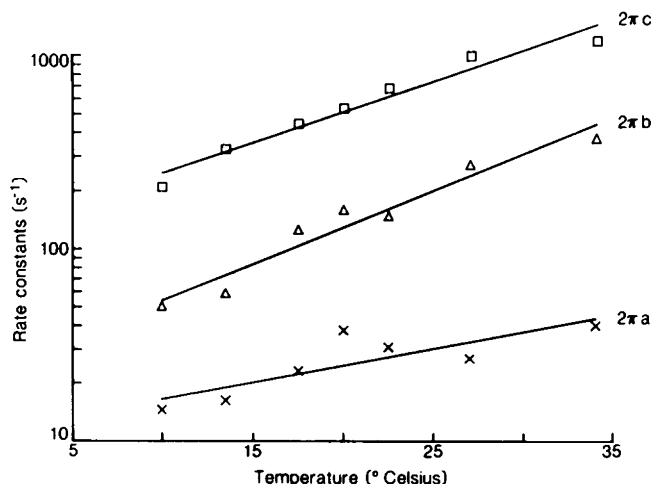
FIGURE 6 Fitted rate constants $2\pi a$, $2\pi b$, and $2\pi c$ from Fig. 5 plotted against temperature. Each process shows a monotonic increase with temperature, and the best fitting straight lines (according to a least mean squares' criteria) were calculated to determine the temperature dependence (Q_{10}).

intermediate- frequency dip (process "B"), and the high-frequency peak (process "C") all shift to higher frequencies with increases in temperature. The depth of the phase dip at intermediate frequencies was maximal for 22.5°C in this experiment, but this was not consistent between experiments. In general, the highest stiffness and the greatest modulation in the phase curve with frequency occurred at the temperature when the tetanic force was highest, often at or slightly above room temperature. Presumably, at that temperature the active force generation produced by cycling of cross-bridges most dominated the properties of passive elements, such as tendons and membranes, which are inevitably present in intact fibers.

The fitted rate constants $2\pi a$, $2\pi b$, and $2\pi c$ are plotted for a range of temperatures in Fig. 6 for a rat EDL fiber bundle. All three rate constants clearly show a monotonic increase with temperature and are widely separated over the range of temperatures studied. The regression lines fitted to the data on the semilogarithmic plots of this figure had correlation coefficients of 0.84, 0.97, and 0.97 for $2\pi a$, $2\pi b$, and $2\pi c$, respectively. From the regression lines the change in rate constant for a 10° change in temperature

(Q_{10}) and the value of the rate constant at 20°C (R_{20}) could be calculated.

Table I summarizes the mean Q_{10} and R_{20} values of each of the three rate processes observed for the sample of rat and mouse EDL bundles studied. Nearly all values of Q_{10} are between 1.8 and 2.4, which would correspond to an apparent enthalpy of activation between 46.8 and 62.0 kJ/mol, if the data were replotted in the form of an Arrhenius plot. The exception was the value for rat EDL (process "B"), which was substantially higher. This value also varied considerably from animal to animal, as indicated by the higher standard deviation, for reasons that remain unclear.

During a period of stimulation the force increased exponentially to a steady tetanic value, and a rate constant for this increase could be measured (see Methods; and Stein et al., 1982). Table I also summarizes the Q_{10} and R_{20} values for the rate of rise of tetanic force. There is remarkably good agreement of both the R_{20} and Q_{10} values between animals. Of particular interest is the similarity between the R_{20} of the rate of tetanus rise and the R_{20} of process "A" (Huxley's phase 4). This process corresponds to the slow exponential increase in force after a sudden step decrease in length (Huxley and Simmons, 1971; see also Hill, 1953), or in the current study, to the low-frequency phase advance seen. Our data suggest that the mechanical equivalent of process "A" may be rate limiting for force development in a tetanus.

Fatigue

Fatigue was induced by stopping the flow of O_2/CO_2 gas to the fiber bundle and repetitively tetanizing the bundle (~ 2 s on and 2 s off). In most cases, at least 120 tetanic contractions were elicited in each of the 18 mouse EDL bundles studied. All experiments were done at room temperature, which varied between 21° and 23°C.

Fig. 7 shows the magnitude and phase of the frequency response of a bundle of mouse EDL fibers, along with the corresponding Nyquist diagrams, at three stages of fatigue. In the top panels, the bundle was completely rested, demonstrated a clear dip at intermediate frequencies of oscillation in both the magnitude and phase, and the Nyquist diagram contained three distinct loops. After 55 tetanic contractions, the magnitude of the stiffness was

TABLE I

TEMPERATURE COEFFICIENTS FOR EDL MUSCLE BUNDLES FROM THE RAT AND MOUSE[*]

Huxley phase	Kawai rate	Rat ($n = 5$)		Mouse ($n = 5$)		Rabbit ($n = 3$)
		Q_{10}	R_{20}	Q_{10}	R_{20}	R_{20}
2	$2\pi c$	1.8 ± 0.3	481 ± 86	1.8 ± 0.2	552 ± 48	820 ± 173
3	$2\pi b$	3.6 ± 1.0	115 ± 25	2.2 ± 0.3	153 ± 38	92 ± 3
4	$2\pi a$	2.0 ± 0.6	27 ± 5	2.4 ± 0.5	21 ± 10	4.4 ± 1
Tet. rise		2.5 ± 0.6	22 ± 8	2.4 ± 0.3	24 ± 6	

All values are means ± standard deviations for the number of experiments indicated.
[*]Compared to published values for skinned EDL fibers in the rabbit (Kawai and Schachat, 1984).
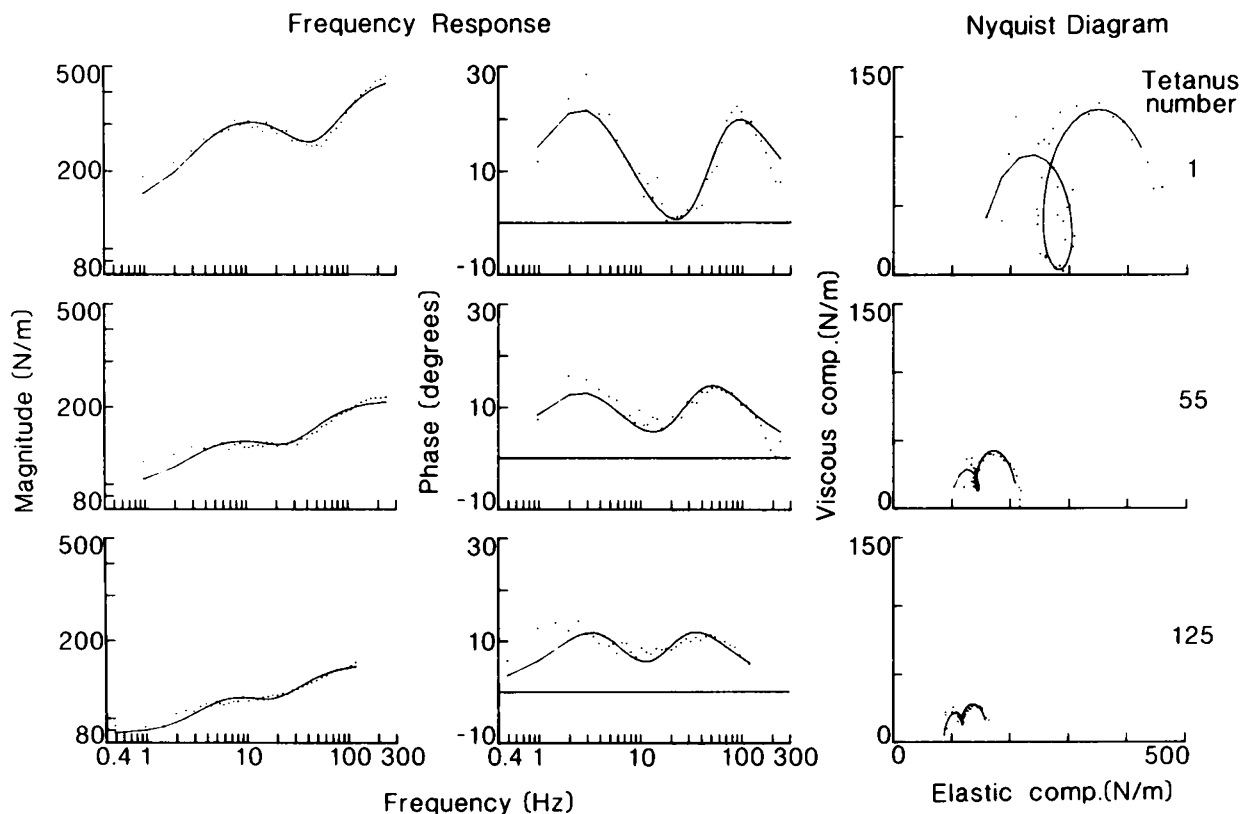
Frequency Response

Nyquist Diagram

FIGURE 7 Frequency-response curves of stiffness, showing magnitude (*left*) and phase (*middle*), and Nyquist diagrams (*right*) for a mouse EDL fiber bundle at the first (*top*), 55th (*middle*), and 125th tetanus (*bottom*). With increases in fatigue, the stiffness declines at all frequencies, and the peak-dip-peak pattern in the phase response, while still visible, tends to flatten out. Both the viscous and elastic components are dramatically affected by fatigue, as shown by the shift towards the origin in the Nyquist diagrams of the points. Close examination of the phase-frequency curves reveals that the frequency of the first peak (a) remains relatively constant with fatigue, but the frequencies of the dip (b) and second peak (c) shift towards lower values with fatigue. Thus the corresponding processes "B" and "C" slow down during fatigue. Tension typically declined to 10–15% of control during the fatigue period.

reduced at all frequencies, and the phase curve was flatter. In addition, while the frequency at which the low frequency peak (process "A") in the phase diagram was unchanged, the frequencies of the intermediate dip and high frequency peak (processes "B" and "C" respectively) both declined in value. The Nyquist diagrams show a large reduction in both the elastic (x-axis) and viscous (y-axis) components of stiffness with fatigue. Furthermore, the "loop" in the plot virtually disappears at the highest tetanus number shown, indicating that process "B" was particularly affected by fatigue.

The effect of fatigue on the rate constants $2\pi a$, $2\pi b$, and $2\pi c$ is summarized in Fig. 8. The mean values and standard deviations for each of these rate constants are plotted for tetanus numbers 1, 6, 15, 30, 50, 80, and 120, based on data from 18 mouse EDL fiber bundles. The rate constants from the rested bundle (tetanus number 1) agree well with the R_{20} values from Table I, after correcting for a slightly higher temperature for bundles from the fatigue study. The rate constants $2\pi b$ and $2\pi c$ declined steadily with increasing number of tetanic contractions. When fitted by standard linear regression analysis on the semilogarithmic plot of Fig. 7, the slopes were significantly
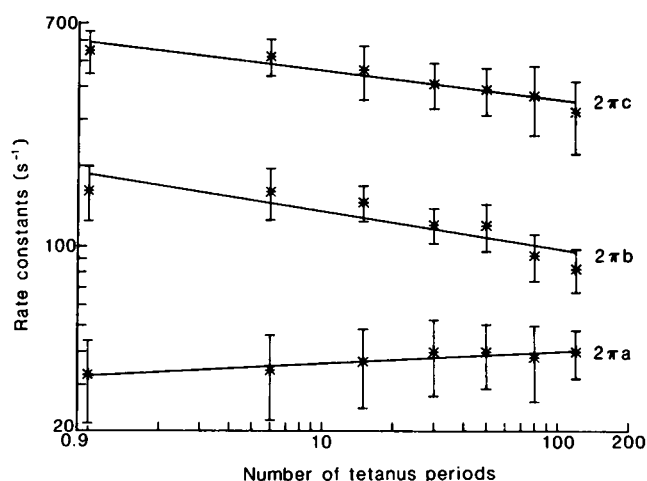
FIGURE 8 Fitted rate constants for each process as a function of the number of stimulation periods. Shown are the mean ± SD values for 18 mouse EDL bundles. When fitted by standard linear regression lines, the rate constants $2\pi b$ and $2\pi c$ showed significant decline with fatigue. No significant effect of fatigue was seen for the rate constant $2\pi a$.

negative (for $2\pi b$ the slope was -0.14 ± 0.03 [mean $\pm$ SE], while for $2\pi c$, the slope was -0.12 ± 0.03). The linear fit is a good first approximation for purposes of statistical testing, but deviations are seen and we don't wish to imply that the rate constants necessarily varied strictly as the logarithm of tetanus number. In contrast, the values of the rate constant $2\pi a$ did not decline and may have increased slightly during fatigue, although the trend was not statistically significant (slope, 0.05 ± 0.04).

DISCUSSION

Our results suggest that contraction in intact mammalian muscle fibers involves at least three mechanical processes at the cross-bridge level, which possess widely different rate constants. These three processes cannot be observed in fibers that are: (a) resting, (b) in the partial, or "low" rigor state, or (c) fixed by the addition of 5% gluteraldehyde. Thus, they appear to reflect dynamic events in the muscle rather than passive properties of the muscle or recording system. Kawai (1978) originally described these processes in skinned mammalian fibers, and we have used his notation in which processes "A", "B," and "C" presumably correspond to those that generate the phases 4, 3, and 2 of Huxley (1974) for single, intact amphibian fibers. The "dip" in the frequency response curve associated with process "B" is much less prominent in slow-twitch muscles such as soleus (Fig. 2 B), as first reported by Kawai and Schachat (1984), so our analysis has been confined to the EDL muscle, which is composed predominately of fast-twitch fibers (Ariano et al., 1973). The reasons for this difference between fast-twitch and slow-twitch muscle fibers are not known.

The advantage of using skinned fibers lies in the ability to vary the concentrations of both metabolites and products, and to examine how these manipulations change the mechanical responses to length perturbations. However, the use of skinned muscle fibers has several drawbacks. These include adding compliance at the points of fiber attachment (Woledge et al., 1985) and along the entire fiber length after membrane removal. Problems of non-uniformity of filament spacing and sarcomere ordering may be encountered in studies using skinned fibers. Such problems are probably less important in intact fiber bundles, where additional connective tissue between adjacent fibers would lead to a more equal distribution of stretches/releases within the bundle (Woledge et al., 1985). Finally, an intact fiber can be excited electrically, so that the time course of tension development and relaxation can be compared with the processes induced by stretch or release. It is important to note that the rate of development of tension upon activation of a skinned fiber preparation is well below that of an intact fiber (Julian and Moss, 1981; Moisescu, 1976; Fabiato and Fabiato, 1978).

Although we have used Kawai's notation for the three processes, based on the qualitatively similar shape of the frequency-response curves, there are some quantitative

differences. In addition to our own data, Table I gives results from Kawai and Schachat (1984), who measured the rate constants for a few skinned rabbit EDL fibers. Our values for the highest rate constant in intact mouse and rat EDL fibers are somewhat lower and our values for the intermediate rate constant are somewhat higher, but the differences can probably be accounted for by species differences, differences in technique, and the fact that the levels of ATP and other important substances probably differ in the intact fiber from those added to the medium bathing a skinned fiber.

A more substantial difference is seen in the slowest rate constant which is five to six times as high in our intact rat and mouse fibers than in the skinned rabbit fibers studied by Kawai and Schachat (1984). Such a discrepancy may reflect the more rapid development of tension in the intact versus the skinned fiber preparation. It is possible that skinning a muscle fiber modifies aspects of the myofilament arrays or their environment, so that some processes are slowed substantially. Certainly, rates can be slowed by an order of magnitude in glycerinated fibers (Cooke and Bialek, 1979), but this discrepancy needs to be investigated further. Abbott and Steiger (1977) measured the temperature dependence of rate constants in rabbit psoas fibers corresponding to processes "B" and "C." They do not give average values, but the Q_{10}'s given for their Fig. 8 A are within the ranges measured here.

What Limits the Rate of Rise of Force in an Isometric Contraction?

There was a close agreement between the slowest rate constant in our experiments ($2\pi a$) and the rate constant for the exponential increase of force to its tetanic levels after the onset of stimulation. In a previous study from this lab (Stein et al., 1982), a good correspondence was found between the rate constant for the exponential decay of tension after a period of stimulation and the rate of uptake of Ca^{2+} ions into the sarcoplasmic reticulum. Therefore, we suggested that the Ca^{2+} ATPase responsible for this process was rate limiting for tension decay. However, no such correspondence was found between the rise of force and the rate of the actomyosin ATPase. We suggested at that time that one process with a relatively low enthalpy of activation limited the rate of rise of force, while another still slower process, but with a higher enthalpy of activation, limited the overall rate of the actomyosin ATPase.

The present results suggest that the rate of rise of force is limited by process "A." Not only is there a good correspondence between the values of the rates at 20°C (R_{20}), but values for the temperature dependence (Q_{10}) and hence the enthalpy of activation are similar. Much the same temperature dependence was reported by Ford et al. (1977) in the frog anterior tibial muscle for their phase 4, which presumably corresponds to process "A." A number of biochemical studies (Taylor, 1979) indicate that the slowest transition between attached states is one associated with release of

products (MgADP and P_i), so we can tentatively link process "A" and the limitation in the rate of rise of force to steps associated with the release of products. During fatigue the rate constant of process "A" did not decline, although the rate constant for the rise of tension decreased (Calancie, B., and R. B. Stein, unpublished observations). An understanding of this discrepancy may require a detailed modelling study of the actomyosin cycle. However, a preliminary analysis (Stein, R. B., unpublished calculations) indicates that, although the rate constant for the rise of tension is numerically close to the value selected for the release of products, several other processes can influence it.

In principle, any process in the chain from electrical excitation to muscular contraction might be rate limiting for force development. Among these events are the release of Ca^{2+} and its binding to troponin. Although there is a delay before the muscle impulse releases Ca^{2+}, the rate of release is fast once it is initiated, based on several Ca^{2+} indicators (Baylor et al., 1982; Cannell and Allen, 1984). Eusebi et al. (1985) recently measured the decay of light generated by aequorin, a Ca^{2+}-sensitive photoprotein, in rat EDL fibers. The Q_{10} was very similar to what we measured for the rate of rise of force, but the rate of decay of the light signals at 20°C was almost twice that measured here for the rate of rise of force.

However, it requires two or three ions of Ca^{2+} to release a single photon from aequorin, so that in the time Ca^{2+} levels dropped to half, the light level would have dropped to a quarter or an eighth. Thus, the decay of free Ca^{2+} is really only a half or a third the value given. Conversely, it is well known that each molecule of troponin can bind a number of Ca^{2+} ions and Hill coefficients of 5 or 6 have been reported, although this could be due to a high degree of cooperativity between a few binding sites (Stephenson and Williams, 1981; Brandt et al., 1984). If several Ca^{2+} ions must bind to a single troponin molecule before tension can be developed, the rate of tension development would be as fast or faster than the decay of light. Furthermore, tension would rise along a distinctly sigmoid curve. Although a slight degree of upward curvature is seen experimentally, the rise of tension is usually well fitted by a single exponential (Stein et al., 1982).

In a recent review article Blinks (1986) concluded that troponin binding of Ca^{2+} was even faster than the decay of the aequorin light signal and was essentially complete before the light began to decay in several muscles. In fact, he suggested that the binding of Ca^{2+} to parvalbumin limited the rate of decay of light and that the release of Ca^{2+} from troponin slowed this decay. Thus, we can probably rule out Ca^{2+} binding to troponin as being rate limiting in the production of tension.

Finally, if process A is indeed involved in determining the rate of rise of tension, rather than a mechanism involving Ca^{2+} binding to troponin, then the rate constant of this process should not be affected by changes in the concentration of calcium. Indeed, Kawai et al. (1981) found that varying the concentration of Ca^{2+} had only a small effect on the apparent rate constant of their process A in activated skinned fiber preparations.

Processes "C" and "B"

The fastest rate constant ($2\pi c$) was also the one that was least temperature dependent with a Q_{10} of 1.8 in both rat and mouse. Ford et al. (1977) found a very similar value ($Q_{10} = 1.85$) for their fastest rate constant (phase 2) in single frog muscle fibers, again suggesting similar mechanisms across various species. However, their initial view was that this process represented a rotation of the cross-bridges between different attached states, rather than an attachment or detachment of cross-bridges. There are now a number of lines of evidence suggesting that this view is not correct. By adding MgATP quickly through the elegant technique of flash photolysis (Goldman et al., 1984a), cross-bridges were detached from the rigor state with a rate constant of 200 s^{-1}. This rate constant continued to increase with increasing maximum MgATP concentration, and its value was measured with an MgATP concentration of 1 mM. The value might be still higher with a higher MgATP concentration (e.g., 5 mM; Goldman et al., 1984b), as it also included the time taken to activate the MgATP by flash photolysis. This time prevented measurements at higher MgATP levels, so the listed value should be considered as a lower limit for the rate occurring under physiological conditions.

In their study of various fast twitch muscles in the rabbit, Kawai and Schachat (1984) found rate constants for their process "C" of 500–900 s^{-1}. The values were also directly dependent on MgATP concentration (Kawai, 1979) and were consistent with the second order rate constant for ATP binding to actomyosin measured biochemically (1.2×10^6 s^{-1} M^{-1}; Lymn and Taylor, 1971; White and Taylor, 1976). It is therefore logical to associate the rate constant $2\pi c$ with the ATP-dependent release of actomyosin bonds from the rigor state. Our finding that this rate decreased dramatically during the course of a fatiguing contraction, which should have severely depleted ATP levels, is consistent with this view.

The intermediate rate constant $2\pi b$ was also greatly decreased by fatigue, but the reason for this decline remains uncertain. A decrease in $2\pi b$ was also found by Kawai (1979) when the MgATP levels bathing skinned muscle fibers were decreased. However, decreased Ca^{2+} levels from impaired activation might also reduce this rate constant (Kawai et al., 1981). Finally, increased osmolality of the muscle fibers and a decrease of pH as a result of lactate accumulation might also contribute. With a reaction scheme as complex as the actomyosin cycle, a thorough modelling study is required to test the effects of various changes in metabolites and products and compare them with observed experimental results. Such a study is in

progress, but a detailed consideration of models would add unduly to the length of the present paper. Furthermore, the experiments described here stand on their own in showing clearly that kinetic analysis can be carried out on intact, mammalian muscle fibers and that the results can be interpreted in terms of some biochemical events underlying contraction. Only by comparing results in intact and skinned preparations can the biochemical events be related to normal physiological processes such as fatigue and changes in muscle temperature during exercise.

REFERENCES

Abbott, R. H., and G. J. Steiger. 1977. Temperature and amplitude dependence of tension transients in glycerinated skeletal and insect fibrillar muscle. *J. Physiol. (Lond.).* 266:13–42.

Ariano, M. A., R. B. Armstrong, and V. R. Edgerton. 1973. Hindlimb muscle fiber populations in five mammals. *J. Histochem. Cytochem.* 21:51–55.

Barden, J. A. 1981. Estimate of rate constants of muscle crossbridge turnover based on dynamic mechanical measurements. *Physiol. Chem. Phys.* 13:211–219.

Barden, J. A., G. H. Rossmanith, and J. Unsworth. 1979. Muscle stiffness in hypertonic solutions. Evidence for changes in rate of crossbridge turnover? *Physiol. Chem. Phys.* 11:317–325.

Baylor, S. M., W. K. Chandler, and M. W. Marshall. 1982. Sarcoplasmic reticulum calcium release in frog skeletal muscle fibres estimated from arsenazo III calcium transients. *J. Physiol. (Lond.).* 344:625–666.

Bendat, J. S., and A. G. Piersol. 1971. Random Data: Analysis and Measurement Procedures. John Wiley & Sons, Inc., New York. 410 pp.

Blinks, J. R. 1986. Sarcoplasmic reticulum function in intact cells: information from intracellular Ca^{++} indicators. *In* The Sarcoplasmic Reticulum. M. Entman and B. Van Winkle, editors. CRC Press, Inc., Boca Raton, FL.

Brandt, P. W., M. S. Diamond, B. Gluck, M. Kawai, and F. Schachat. 1984. Molecular basis of cooperativity in vertebrate muscle thin filaments. *Carlsberg Res. Commun.* 49:155–167.

Calancie, B., and R. B. Stein. 1985. The effect of fatigue on the contraction kinetics of intact, fast-twitch mammalian muscle fibers. *Physiologist.* 28:320.

Cannell, M. B., and D. G. Allen. 1984. Model of calcium movements during activation in the sarcomere of frog skeletal muscle. *Biophys. J.* 45:913–925.

Cooke, R., and W. Bialek. 1979. Contraction of glycerinated muscle fibers as a function of the MgATP concentration. *Biophys. J.* 28:241–259.

Cooke, R., and E. Pate. 1985. The effects of ADP and phosphate on the contraction of muscle fibers. *Biophys. J.* 48:789–798.

Cooley, J. W., and J. W. Tukey. 1965. An algorithm for the machine calculation of complex Fourier series. *Math. Comput.* 19:297–301.

Cox, R. M., and M. Kawai. 1981. Alternate energy transduction routes in chemically skinned rabbit psoas muscle fibres: a further study of the effect of MgATP over a wide concentration range. *J. Muscle Res. Cell Motil.* 2:203–214.

Eisenberg, E., and T. L. Hill. 1985. Muscle contraction and free energy transduction in biological systems. *Science (Wash. DC).* 227:999–1006.

Eusebi, F., R. Miledi, and R. Takahashi. 1985. Aequorin-calcium transients in mammalian fast and slow muscle fibers. *Biomed. Res.* 6:129–138.

Fabiato, A., and F. Fabiato. 1978. Effects of pH on the myofilaments and the sarcoplasmic reticulum of skinned cells from cardiac and skeletal muscles. *J. Physiol. (Lond.).* 276:233–255.

Ford, L. E., A. F. Huxley, and R. M. Simmons. 1977. Tension responses to sudden length change in stimulated frog muscle fibres near slack length. *J. Physiol. (Lond.).* 269:441–515.

French, A. S., and A. V. Holden. 1971. Alias-free sampling of neuronal spike trains. *Kybernetik.* 8:165–171.

Goldman, Y. E., M. G. Hibberd, and D. R. Trentham. 1984a. Relaxation of rabbit psoas muscle fibres from rigor by photochemical generation of adenosine-5'-triphosphate. *J. Physiol. (Lond.).* 354:577–604.

Goldman, Y. E., M. G. Hibberd, and D. R. Trentham. 1984b. Initiation of active contraction by photogeneration of adenosine-5'-triphosphate in rabbit psoas muscle fibres. *J. Physiol. (Lond.).* 354:605–625.

Hibberd, M. G., J. A. Dantzig, D. R. Trentham, and Y. E. Goldman. 1985. Phosphate release and force generation in skeletal muscle fibers. *Science (Wash. DC).* 228:1317–1319.

Hill, A. V. 1953. The mechanics of active muscle. *Proc. R. Soc. Lond. B Biol. Sci.* 141:104–117.

Huxley, A. F. 1974. Muscular contraction. *J. Physiol. (Lond.).* 243:1–43.

Huxley, A. F., and R. M. Simmons. 1971. Proposed mechanism of force generation in striated muscle. *Nature (Lond.).* 233:533–538.

Julian, F. J., and R. L. Moss. 1981. Effects of calcium and ionic strength on shortening velocity and tension development in frog skinned muscle fibers. *J. Physiol. (Lond.).* 311:179–199.

Kawai, M. 1978. Head rotation or dissociation? A study of exponential rate processes in chemically skinned rabbit muscle fibers when MgATP concentration is changed. *Biophys. J.* 22:97–103.

Kawai, M. 1979. Effect of MgATP on cross-bridge kinetics in chemically skinned rabbit psoas fibers as measured by sinusoidal analysis technique. *In* Cross-bridge Mechanisms in Muscle Contraction. H. Sugi and G. H. Pollack, editors. University of Tokyo Press, Tokyo. 149–169.

Kawai, M. 1982. Correlation between exponential processes and cross-bridge kinetics. *In* Basic Biology of Muscle: A Comparative Approach. B. M. Twarog, R. J. C. Levine, and M. M. Dewey, editors. Raven Press, New York. 109–130.

Kawai, M., and P. W. Brandt. 1976. Two rigor states in skinned crayfish single muscle fibers. *J. Gen. Physiol.* 68:267–280.

Kawai, M., and P. W. Brandt. 1980. Sinusoidal analysis: a high resolution method for correlating biochemical reactions with physiological processes in activated skeletal muscles of rabbit, frog and crayfish. *J. Muscle Res. Cell Motil.* 1:279–303.

Kawai, M., P. W. Brandt, and M. Orentlicher. 1977. Dependence of energy transduction in intact skeletal muscles on the time in tension. *Biophys. J.* 18:161–172.

Kawai, M., R. N. Cox, and P. W. Brandt. 1981. Effect of Ca ion concentration on cross-bridge kinetics in rabbit psoas fibers. Evidence for the presence of two Ca-activated states of thin filament. *Biophys. J.* 35:375–384.

Kawai, M., and F. H. Schachat. 1984. Differences in the transient response of fast and slow skeletal muscle fibers. *Biophys. J.* 45:1145–1151.

Kawai, M., and M. I. Schulman. 1985. Crossbridge kinetics in chemically skinned rabbit psoas fibres when the actin-myosin lattice spacing is altered by dextran T-500. *J. Muscle Res. Cell Motil.* 6:313–332.

Lymn, R. W., and E. W. Taylor. 1971. Mechanism of adenosine triphosphate hydrolysis by actomyosin. *Biochemistry.* 10:4617–4624.

Moisescu, D. G. 1976. Kinetics of reaction in calcium-activated skinned muscle fibers. *Nature (Lond.).* 262:610–613.

Parmiggiani, F., R. B. Stein, and R. Rolf. 1981. Slow changes and Wiener analysis of nonlinear summation in contractions of cat muscles. *Biol. Cybern.* 42:177–188.

Ruegg, J. C., H. J. Kuhn, K. Guth, G. Pfitzer, and F. Hofmann. 1984. Tension transients in skinned muscle fibres of insect flight muscle and mammalian cardiac muscle: effect of substrate concentration and treatment with myosin light chain kinase. *In* Contractile Mechanisms in Muscle. G. H. Pollack and H. Sugi, editors. Plenum Publishing Corp., New York. 605–615.

Shimizu, H., and H. Tanaka. 1984. Symmetric and asymmetric processes in the mechano-chemical conversion in the cross-bridge mechanism studied by isometric tension transients. *In* Contractile Mechanisms in Muscle. G. H. Pollack and H. Sugi, editors. Plenum Publishing Corp., New York. 585–599.

Stein, R. B., T. Gordon, and J. Shriver. 1982. Temperature dependence of mammalian muscle contractions and ATP activities. *Biophys. J.* 40:97–107.

Stein, R. B., R. Rolf, and B. Calancie. 1986. Improved methods for studying the mechanical properties of biological systems with random length changes. *Med. & Biol. Eng. & Comput.* 24:292–300.

Stephenson, D. G., and D. A. Williams. 1981. Calcium-activated force responses in fast and slow twitch skinned muscle fibres of the rat at different temperatures. *J. Physiol. (Lond.).* 317:281–302.

Taylor, E. W. 1979. Mechanism of actomyosin ATPase and the problem of muscle contraction. *Chem. Rubber Co. Crit. Rev. of Biochem.* 6:103–164.

White, H. D., and E. W. Taylor. 1976. Energetics and mechanism of actomyosin adenosine triphosphatase. *Biochemistry.* 15:5818–5826.

Woledge, R. C., N. A. Curtin, and E. Homsher. 1985. Energetic aspects of muscle contraction. Monographs of the Physiological Society, No.41. Academic Press, London. 359 pp.